

Detrended Fluctuation Analysis of Systolic Blood Pressure Control Loop

C.E.C. Galhardo¹, T.J.P.Penna¹, M. Argollo de Menezes¹ and P.P.S. Soares²

¹ Instituto de Física, Universidade Federal Fluminense, Av. Litoranea, s/n, 24210-340, Niteroi, RJ, Brazil

² Instituto Biomédico, Universidade Federal Fluminense, R. Prof. Hernani Melo n. 101, 24210-130, Niteroi, RJ, Brazil

Abstract. We use detrended fluctuation analysis (DFA) to study the dynamics of blood pressure oscillations and its feedback control in rats by analyzing systolic pressure time series before and after a surgical procedure that interrupts its control loop. We found, for each situation, a crossover between two scaling regions characterized by exponents that reflect the nature of the feedback control and its range of operation. In addition, we found evidences of adaptation in the dynamics of blood pressure regulation a few days after surgical disruption of its main feedback circuit. Based on the paradigm of antagonistic, bipartite (vagal and sympathetic) action of the central nerve system, we propose a simple model for pressure homeostasis as the balance between two nonlinear opposing forces, successfully reproducing the crossover observed in the DFA of actual pressure signals.

PACS numbers: 05.40.-a,87.19.Hh,87.80.Vt,89.75.Da

Submitted to: *New J. Phys.*

1. Introduction

Negative feedback loops are ubiquitous in living systems, with important examples like the lac-operon in gene regulation [1], which inhibits lactose consumption in the presence of glucose, and serve as efficient ways of maintaining stability and suppressing fluctuations in noisy environments [2, 3, 4, 5, 6] ‡. On a much larger physical scale, the autonomous nerve system is able to sustain (without external supervision) basic life signals like temperature, water and metabolite concentrations at safe levels by the action of a pair of nerve branches, called sympathetic and parasympathetic (or vagal). These nerve branches have cooperative and “antagonistic” roles in our body: while the sympathetic prepares our body for “flight-or-fight” situations (increasing heart rate, dilating pupils and cancelling digestive functions, for instance), the vagal, or parasympathetic, decreases heart rate, constricts pupils and stimulate salivary glands. The balance between these “forces”, which keeps living systems operating close to optimal levels, is called *homeostasis* [8, 9]. Alterations of a given control mechanism can perturb such balance and lead to pathological conditions such as Diabetes Mellitus, which results from a malfunctional insulin metabolism [6].

A major feature of the autonomous nerve system is that stimulation of the vagal branch results in a inhibition of the sympathetic branch, which acts continuously on organs and veins at an approximately steady level when not inhibited. These nerve branches are controlled at the Nucleus Tractus Solitarius (NTS) of the medulla by integration of neural information coming from afferent neural fibers, which carry information from sensory neurons spread around the body. Among other sensory information carried by those fibers, one of utmost importance regards arterial blood pressure: through these afferent nerve fibers, stretch-sensitive mechanoreceptors spread around veins and arteries of the heart return to the NTS (in a timescale of few seconds) information about the current status of pressure (and its variation). † The NTS, in turn, excite (when pressure is high) or inhibit (when pressure is low) the vagal branch, closing the circuit for what can be regarded as a self-inhibitory feedback loop called *baroreflex* [8, 9, 11] (See figure 1).

As a result of this balance the body, although continuously perturbed by external factors, is able to keep homeostasis, a stationary state where, among other things, arterial pressure, temperature, water and metabolite concentrations are kept at optimal levels [8, 9]. One can think of homeostasis as a locally optimal state sustained by feedback loops in a noisy environment. The reasonably controlled flow of nutrients throughout veins and arteries is achieved with the aid of the blood system and the heart, whose pumping action is monitored and controlled by the autonomous

‡ Negative feedback loops also appear in electronic circuits as a tool for the stabilization of laser beams (see [7])

† There are also baroreceptors at the kidneys, which change body fluid volume at the timescale of hours or days [10]. Those are responsible for very low frequency fluctuations and will not be analyzed here.

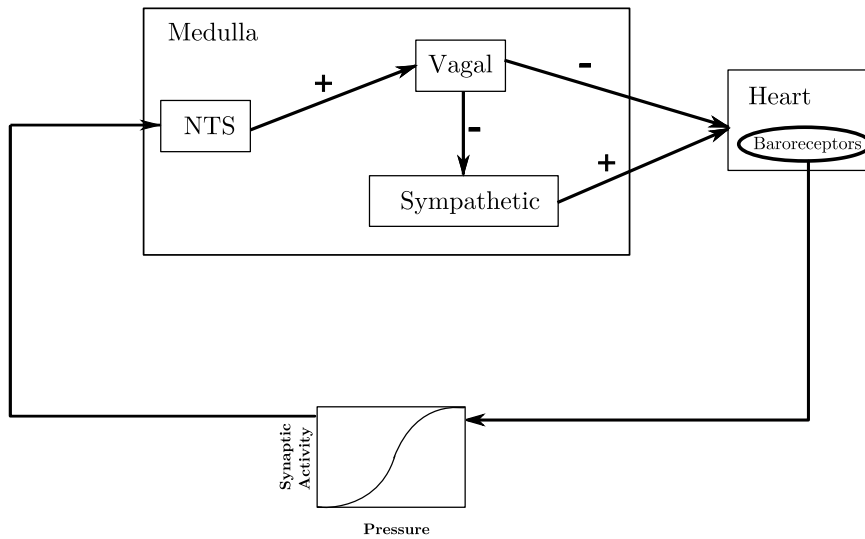


Figure 1. Schematics of the negative feedback loop for pressure control, or baroreflex. Stimulus from afferent neurons excite the vagal branch of the autonomous nerve system, which in turn slows down heart rate. At the same time, the sympathetic branch, which acts to increase heart rate, is inhibited by the vagal branch. As a result, a surge in blood pressure tends to stimulate the vagal branch and inhibit the sympathetic branch, decreasing heart rate and, consequently, decreasing blood pressure.

nerve system. Arterial blood pressure (ABP) is one of the vital signals that can be continuously monitored, which carries a large amount of information about the mechanisms responsible for homeostasis and the different timescales for their responses [12, 13]. Given a continuous set of recordings of ABP, $\{p(t)\}$, over a given period of time, one defines the n -th diastolic blood pressure as the n -th local minimum p_n , the systolic blood pressure as the n -th local maximum p_n and the time interval between two neighboring ABP minima, $b_n = t(p_{n+1}) - t(p_n)$, as the instantaneous inter-beat heart rate (IR), as depicted in figure 2.

These quantities have long been characterized by spectral methods [14, 15], where peaks in the power spectrum $S_\omega = \left| \frac{1}{2\pi} \sum b_n e^{i\omega n} \right|^2$ reveal the timescales for the response of different control mechanisms [16, 17, 18, 19, 20]. Nevertheless, in order to assess the long-range correlations [21] emerging from these feedback control systems, or to characterize disruptive and abnormal states, one must recur to methods which account for the strong non-stationarity of those signals [22], such as detrended fluctuation analysis (DFA) [23, 24, 25, 26, 27, 28, 29]. In this work we analyze the dynamics of baroreflex, the negative feedback loop providing a rapid and powerful reflex control of blood pressure, which is by far the most studied cardiovascular reflex in physiological and clinical settings. For such purpose we apply DFA to experimental time series consisting of continuous arterial systolic blood pressure measurements.

We report results of experiments on rats with surgical disruption of the nerve fibers connecting the baroreceptors to the medulla, a procedure called sinoaortic denervation (SAD) [30], and find that other mechanisms might be responsible for arterial blood

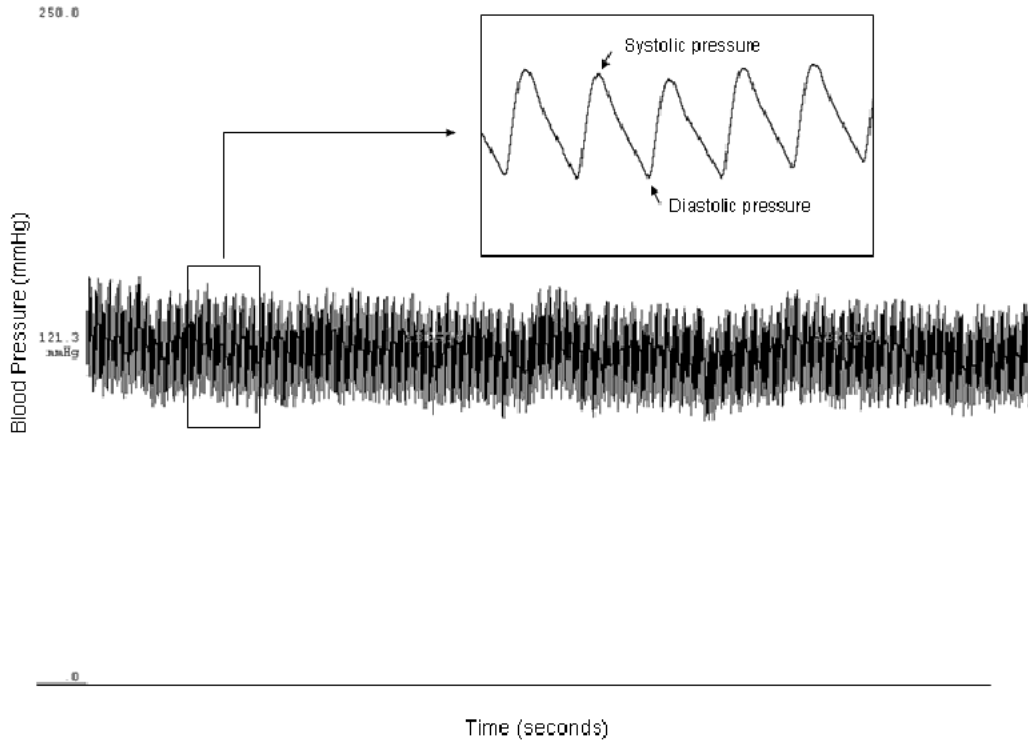


Figure 2. Time evolution of arterial blood pressure (ABP). The local maxima are called systolic blood pressure, the minima are the diastolic pressure and the time interval between two neighboring ABP minima is the instantaneous inter-beat heart rate. In this work we focus on the arterial systolic blood pressure and its variation in time.

pressure control, although at different time scales, possibly due to synaptic plasticity at the NTS [31, 32, 33]. Following this recovery, average blood pressure is kept at almost the same levels as before denervation, a determinant condition for the kidneys to work properly [8, 9]. We apply detrended fluctuation analysis to our experimental time series and find that fluctuations in systolic blood pressure cross over from non-stationary to stationary, long-range correlated at a characteristic time scale τ . Surgical denervation of baroreceptors significantly changes the correlation patterns of pressure signals but, after 20 days, correlation patterns typical of non-operated rats are recovered, only with larger crossover times $\tau' > \tau$. This suggests that the control loop is reestablished, possibly due to adaptation to sensory information coming from other less effective receptors.

To model such feedback control loop we develop a model of a random walker forced by two opposing nonlinear (sigmoidal) forces, representing the sympathetic action and its inhibition by the vagal (parasympathetic) branch. We find the same crossover from non-stationary to stationary, long-range correlated noise observed in actual pressure measurements. Moreover, by changing the difference between the sensitivity of each branch, we find the same shift in the crossover time scale, as observed in rats 20 days after surgery, when adaptation occurs and homeostasis is recovered.

2. Experiments and Measurements

Adult male Wistar rats were maintained on a 12-hour light/dark lighting schedule at 23°C, food and water *ad libitum*. All procedures were performed according to [34]. The animals were divided in three groups: control rats (ctr, $N = 11$ rats), acute sinoaortic denervated rats (1d, $N = 5$ rats), i.e, animals surgically denervated one day before measurements, and chronic sinoaortic denervated rats (20d, $N = 8$ rats), animals surgically denervated 20 days before measurements. SAD was performed using the methods described by Krieger et al [35], and basically consists of full disruption of the nerve fibers connecting the baroreceptors spread in veins and arteries of the heart to the medulla. Blood pressure was recorded from the left femoral artery for 90 minutes in conscious rats. Before the analog to digital conversion, blood pressure was low-pass filtered ($f_c = 50$ Hz) for high-frequency noise removal, and recorded with a 2kHz sampling frequency. Systolic (maximum) and diastolic (minimum) values were detected after parabolic interpolation and signal artifacts were visually identified and removed. Pulse intervals were measured in milliseconds (ms), considering intervals between consecutive diastole and the heart rate was calculated as the inverse of pulse interval and measured in beats per minute (bpm) (A more detailed account of this experiment can be found in [36]). Since the measurements were made in awake, conscious unrestrained rats, some distortions in the blood pressure signal might arise due to their movements. To reduce this problem we discard series that show any kind of discontinuities or jumps. After this selection we keep six time series for the control group, five time series for the chronic denervated group and four time series for the acute denervated group. Each time series consists of 10^4 data points, equivalent to 30 minutes of continuous measurements.

In figure 3 we depict the series of systolic blood pressure values for the three groups: while pressure in non-operated rats fluctuates in a stationary fashion about 116.55 ± 10.15 mm Hg (Figure 3a), it is non-stationary in rats with disrupted baroreflex (Figure 3b), fluctuating about a much higher average value of 178.31 ± 31.15 mm Hg. After a period of 20 days, average blood pressure falls back to safe levels, 129.95 ± 9.32 mm Hg, and fluctuations are again stationary (Figure 3c), indicating that baroreflex is recovered. In order to understand the underlying principles behind blood pressure regulation and the sources of fluctuations in blood pressure levels we give, in the next section, a precise, quantitative meaning to such fluctuations with detrended fluctuations analysis (DFA).

3. Fluctuation Analysis and Computer Modelling

We used detrended fluctuation analysis (DFA) [25, 23] to characterize long term correlations in arterial systolic blood pressure. This method has been successfully applied to analyze diverse non-stationary physiological signals [37, 38, 25, 26, 27, 28] and we briefly describe it in the following: Let $\{P(t)\}$ be the systolic blood pressure

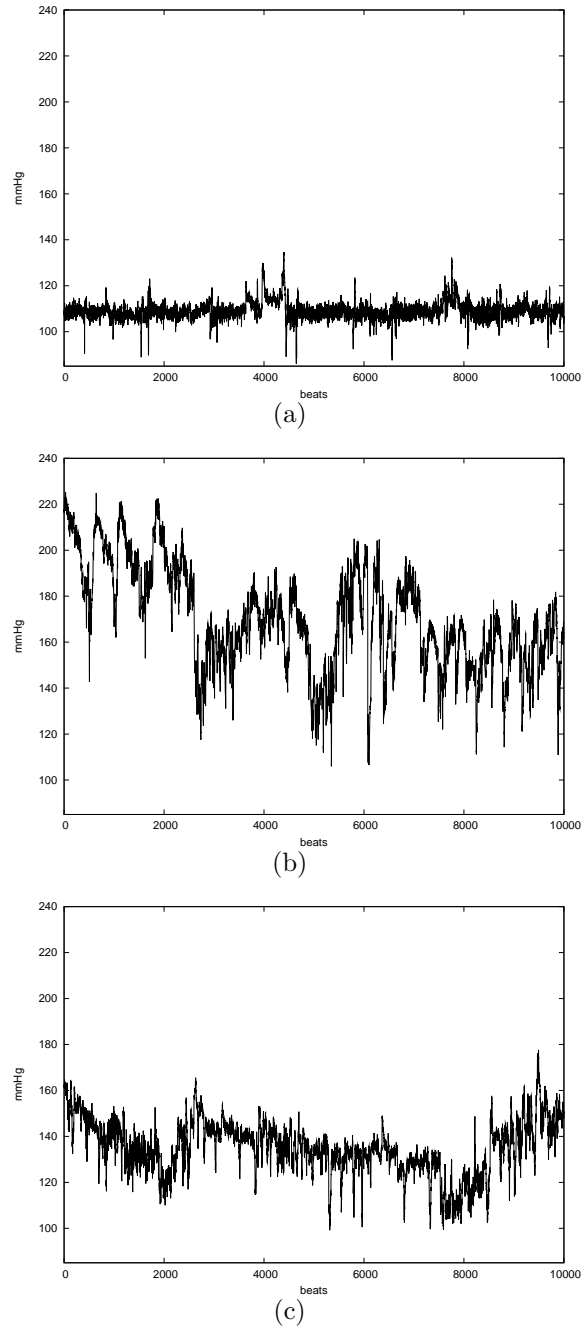


Figure 3. (a) Fluctuations of arterial systolic blood pressure from a rat in the control group. Blood pressure oscillates about safe, steady levels. (b) One day after disrupting the pressure control loop with a surgical procedure, pressure fluctuates in a non-stationary fashion, reaching dangerously high values. (c) As a result of physiological adaptation, 20 days after surgical denervation of baroreceptors average blood pressure returns to safe levels and fluctuations are again stationary.

time series and P_{ave} its time average. Define the integrated time series $\{y(t)\}$ with

$$y(t) = \sum_{k=1}^t (P(k) - P_{ave}) \quad (1)$$

Divide the integrated series in boxes of equal sizes n and, for each box, calculate the detrended profile subtracting from the original signal a l -degree polynomial least-squares fit, $y_n^l(t)$ (In the following DFA- l will stand for detrended fluctuation analysis with l -degree polynomials [39]). At each box of size n , calculate the fluctuation

$$F(n) = \sqrt{\frac{1}{N} \sum_{t=1}^N (y(t) - y_n^l(t))^2}. \quad (2)$$

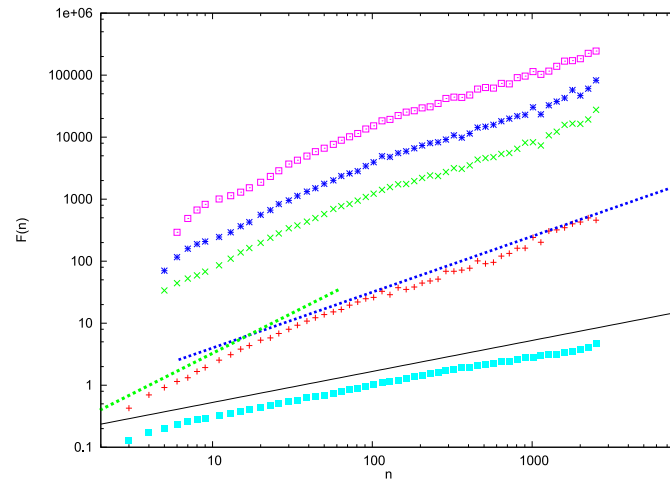
A power-law relation $F(n) \sim n^\alpha$ implies different correlation patterns for different values of α : When $0 < \alpha < 1/2$ the signal is stationary and long-range anti-correlated, with $\alpha = 1/2$ for a white noise (and $\alpha = 3/2$ for its integral, the Brownian motion), $\alpha > 1/2$ for long-range correlated signals, while the paradigmatic $1/f$ noise corresponds to $\alpha = 1$. This value of α also marks the borderline between stationary and non-stationary behavior: For $\alpha \geq 1$ one has non-stationary signals, with sub-diffusive ($\alpha < 3/2$), diffusive ($\alpha = 3/2$) or super diffusive ($\alpha > 3/2$) behavior.

Results for a typical time series from the control group are depicted in figure 4a. With DFA-1 we obtain a crossover from $\alpha = 1.18$ to $\alpha = 0.93$ at $n \approx 35$. To check that the crossover is not an artifact of a specific polynomial fit or non-stationarities [40, 24, 41], we also employed DFA-2, DFA-3 and DFA-4 on the time series. For all orders l there is a crossover, although at slightly shifted time scales. We also show surrogate data, where data points are randomly shuffled, and applied DFA-1 to it (Figure 4a, bottom curve) to find that fluctuations scale with $\alpha \approx 0.5$, as in a typical white noise. We depict in figure 4b results for all rats in the control group, evidencing the same behavior in all curves.

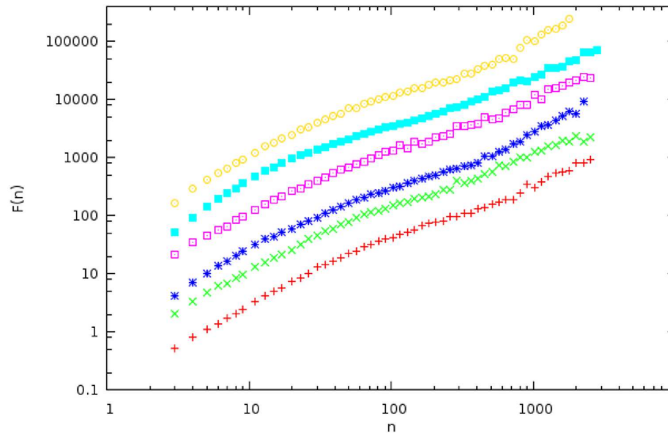
With sinoartical denervation stationarity is lost, as DFA indicates (Figure 5). On pressure series from rats analyzed 24 hours after denervation (acute group) the crossover disappears, and the series is non-stationary at all time scales ($\alpha \approx 1.25$), severely affecting homeostatic regulation of blood pressure. Again we use higher order DFA check that no trends or non-stationarities are shaping the results. The surrogate test is also shown at the bottom curve of figure 5a.

It is interesting to note that the same change of behavior has been observed in the DFA analysis of fluctuations in blood glucose levels of healthy humans and in patients with Diabetes Mellitus [6]: The damaged insulin metabolism controlling blood sugar levels is reflected in the disappearance of the crossover observed in the DFA curves of healthy subjects. In other study [42], this has been connected to the loss of short-term adaptability of the cerebral blood flow control system of migraineurs patients.

Twenty day past the denervation procedure, average blood pressure returns to safe levels and stationarity is recovered (Figure 6): there is again a crossover from non-stationary ($\alpha \approx 1.42$) to stationary ($\alpha \approx 0.99$) fluctuations, although at a larger timescale $n \approx 100$. Again we use DFA-1 up to DFA-4 to insure that the crossover is not an artifact of nonstationarities (Figure 6a) and depict in figure 6b results for each rat in the chronic group. The average blood pressure and the stationary, long-range correlated fluctuations (as measured by α in the region after the crossover) are



(a)



(b)

Figure 4. (a) Detrended fluctuation analysis of systolic blood pressure time series for a typical rat in the control group. There is a crossover from non-stationary to stationary, long-range correlated behavior at $n \approx 35$: For short time scales we have $\alpha \approx 1.18$ and for large time scales $\alpha \approx 0.93$. We apply DFA-1 (red crosses), DFA-2 (green times), DFA-3 (blue stars) and DFA-4 (pink empty squares) to the series and find that the crossover always exists, although at different scales. We also applied DFA-1 to shuffled data (bottom curve), for which $\alpha \approx 0.5$ as for a white noise. (b) DFA-1 for all rats in the control group. In both figures curves are shifted vertically for better visibility. The curves $y = Ax^\alpha$ with $\alpha = 0.5$ (full black line), 0.9 (dashed blue line) and 1.3 (dashed green line) are plotted as guides to the eye.

statistically equivalent, as summarized in figure 7. When comparing the exponent α in the control and chronic groups with a paired t-test [43] we find statistical equivalence with p-value $p = 0.04$, the same test for average blood pressure giving $p = 0.07$.

Baroreflex recovery can be associated to the adaptation of sensory neurons, most possibly at the Nucleus Tractus Solitarius (NTS) [31, 32, 33] (the mechanisms underlying this learning or synaptic plasticity are not completely understood, but are already

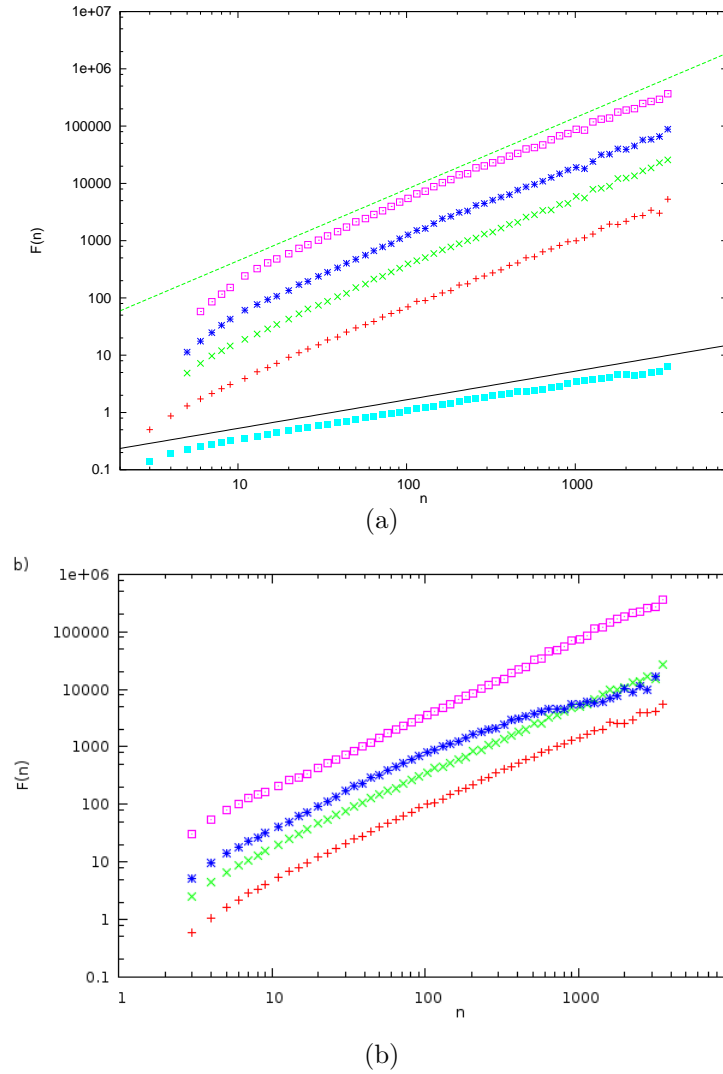


Figure 5. (a) Detrended fluctuation analysis of systolic blood pressure time series for a typical rat in the acute group. One day past surgical denervation of baroreceptors, fluctuations in blood pressure are non-stationary at all time scales and there is no crossover in the $F(n)$ curve. We apply DFA-1 (red crosses), DFA-2 (green times), DFA-3 (blue stars) and DFA-4 (pink empty squares) and find $\alpha \approx 1.25$, indicating a disruption of short-term homeostatic control of blood pressure, or baroreflex. We also applied DFA-1 to shuffled data (bottom curve, full squares), for which $\alpha \approx 0.5$ as for white noise. (b) DFA-1 for all rats in the acute group. In both figures curves are shifted vertically for better visibility. The curves $y = Ax^\alpha$ with $\alpha = 0.5$ (full black line) and 1.25 (dashed green line) are plotted as guides to the eye.

present in the adaptation of stretch sensitivity in baroreceptors during the execution of simple tasks such as sitting or head tilting for a reasonable amount of time [44]). In rats with intact baroreceptors, baroreflex sensitivity can be evaluated, both with vasoactive drugs or by spontaneous fluctuations of heart rate and blood pressure, by means of the *Oxford method* [45]: Beat-to-beat variation of systolic blood pressure is plotted against variation of the heart rate at the subsequent beat interval. The slope

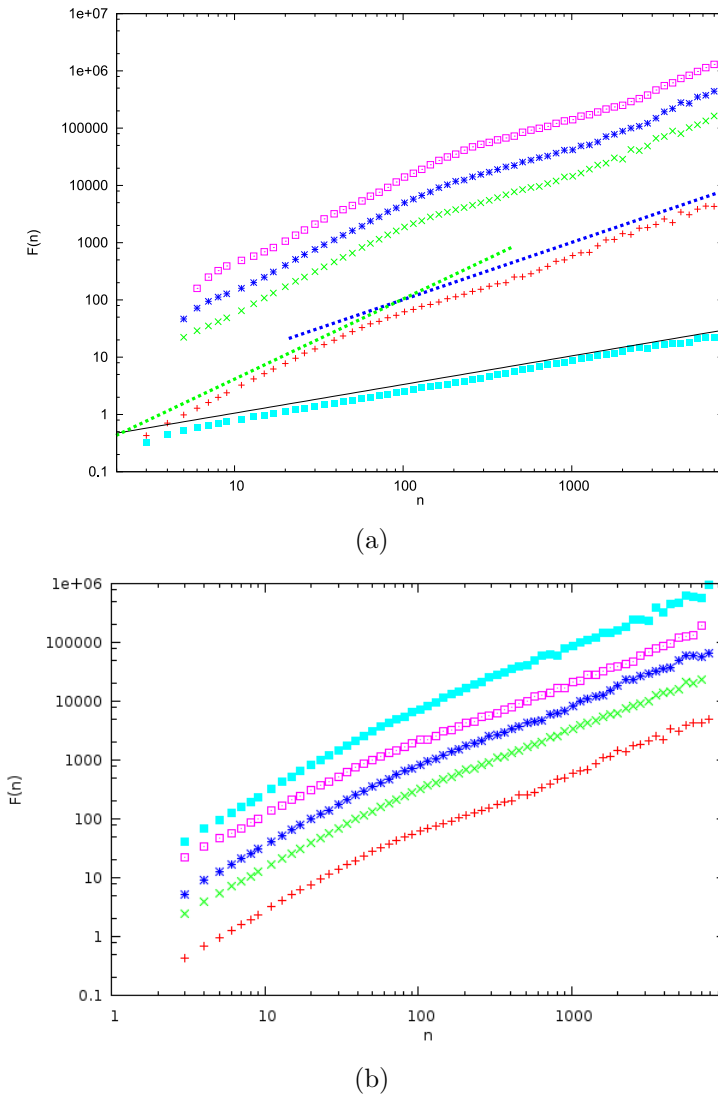


Figure 6. (a) Detrended fluctuation analysis of systolic blood pressure time series for a typical rat in the chronic group: 20 days after surgical denervation, stationarity is recovered at large timescales and fluctuations cross over from non-stationary ($\alpha \approx 1.42$) to stationary, long-range correlated ($\alpha \approx 0.99$) at $n \approx 100$. This result suggests that, although the fast response from the baroreceptors in the heart is lost, physiological adaptation reestablishes homeostatic regulation. We apply DFA-1 (red crosses), DFA-2 (green times), DFA-3 (blue stars) and DFA-4 (pink empty squares) to the series and find that the crossover always exists, although at different scales. We also applied DFA-1 to shuffled data (bottom curve), for which $\alpha \approx 0.5$ as in white noise. (b) DFA-1 for all rats in the chronic group. In both figures curves are shifted vertically for better visibility. The curves $y = Ax^\alpha$ with $\alpha = 0.5$ (full black line), 1.0 (dashed blue line) and 1.4 (dashed green line) are plotted as guides to the eye.

of a linear regression of this relation provides an index of arterial baroreflex sensitivity (the same measure can be achieved by correlating blood flow and heart rate variation and is known as the *Trieste method* [46]). These methods assume that the two signals are coupled, mostly at oscillatory frequencies of 0.4 Hz [47] and give a sigmoidal-like

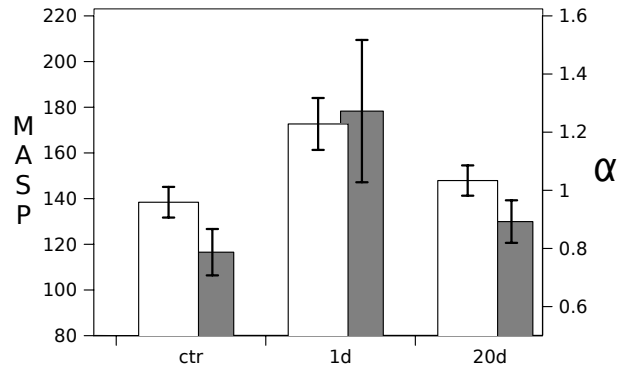


Figure 7. Results for the mean arterial systolic pressure (MASP) (light gray bars) and the exponent α of long-term fluctuations averaged over all rats in each group, showing homeostasis adaptation of mean pressure and its fluctuations. In the control group (ctr), MASP have basal levels of 116.55 ± 10.15 mm Hg. One day after denervation (1d), MASP rises to 178.31 ± 31.15 mm Hg and, after 20 days (20d), get back to a basal level of 129.95 ± 9.32 , closer to basal levels of the control group. The long-range correlations observed both in control and chronic groups are statistically equivalent ($\alpha = 0.96 \pm 0.05$ for the first and $\alpha = 1.03 \pm 0.05$ for the latter group) with p-value $p = 0.04$. Acute (1d) denervated rats have nonstationary fluctuations, with $\alpha = 1.23 \pm 0.09$ on all timescales.

relation between afferent nerve activity and blood pressure [48, 44]. In order to model the action of both vagal and sympathetic branches on blood pressure we devise a model of a Brownian particle forced by opposing nonlinear forces, an idea briefly touched upon in [49]. Pressure information merges through afferents and is integrated at the NTS, stimulating the vagal branch, which further inhibits the sympathetic branch of the autonomous nerve system. This coupled action can be modelled by sigmoidal-like pressure-activity curves, as depicted in figure 8: at each time step, pressure changes due to the action of the forces $f_v(p)$ and $f_s(p)$ as

$$p(t+1) = p(t) + (f_s(p + \xi(t)) - f_v(p + \xi(t))) \quad (3)$$

where $\xi(t)$ represents the background noise integrated together with afferent signal at the NTS, and the response curve $f_k(p)$ is modeled by sigmoid-like curves [48, 44]:

$$f_k(p) = A_k \pm \frac{1}{B_k + e^{-(p-thr_k)}} \quad (4)$$

where $k = s, v$ stands for sympathetic and vagal, respectively. In the first case one subtracts and in the latter one adds the sigmoidal curve to the base level of operation of each branch, called *tone*, represented by A_k . The parameters thr_s and thr_v give the pressure values for the optimal response of each branch: the more different they are the larger is the region where pressure fluctuates randomly. In order to understand the role of the antagonistic regulation of average blood pressure in our model, we arbitrarily set $A_v = 0.1$, $A_s = 1.0$, $B_v = 1.1$ and $B_s = 1.0$. ‡

‡ One could simplify the problem substituting the sigmoidal forces by step functions. We chose, however, to keep the biologically motivated sigmoidal responses.

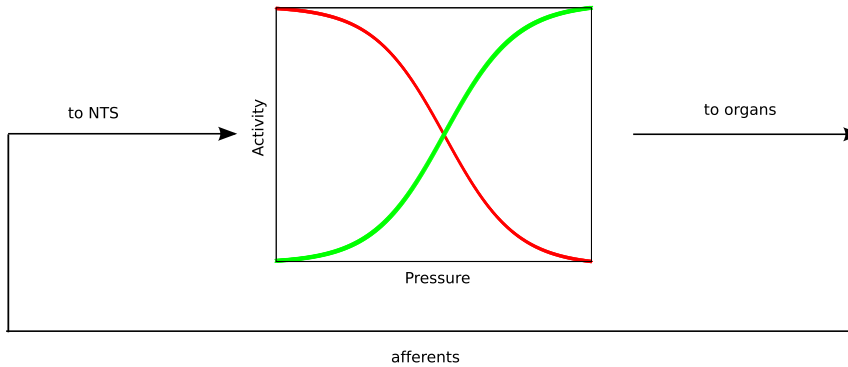


Figure 8. To model homeostatic blood pressure control we propose a simple model of a Brownian particle driven by noisy sigmoidal antagonistic forces f_s (in red) and f_v (in green). Pressure information is sent through afferents to the NTS of the medulla, stimulating the vagal branch in a sigmoid fashion (green curve). The otherwise constant action of the sympathetic branch is modified by its vagal inhibition, resulting in the red curve depicted above. The equilibrium condition $f_s = f_v$ sets the average pressure.

We analyze artificial systolic blood pressure series generated by such forced random walk with DFA. After some transient behavior we store a time series $\{p(t)\}$ with the same number of points as the experimental datasets, $T = 10^4$. We find, with this simple model, the same crossover observed in the actual pressure time series of intact rats from the control group. Moreover, keeping the same mechanism for pressure control, but changing the sensitivity difference $thr_s - thr_v$, we are able to reproduce the increase in the crossover scale observed in chronic SAD rats (figure 9).

This result can be understood by the following simple argument: substituting the sigmoidal curves by step functions, the problem reduces to one of a particle in a confining square-well potential of width $L \approx thr_s - thr_v$. The first-passage-time of the random walker to the walls of the potential sets a timescale for a crossover between random, non-stationary fluctuations and confined motion [50]. Thus, with an increase of the width of the potential well one should expect an increase of the range of the scaling region related to non-stationary fluctuations.

4. Discussion

We analyzed the dynamics of baroreflex, the negative feedback loop providing reflex control of blood pressure by the autonomous nerve system, with detrended fluctuation analysis of continuous measurements of arterial systolic blood pressure. We report results of our experiments with three groups of rats: a control group, another group where baroreflex is surgically disrupted one day before measurements and a third one, again with baroreflex surgically impaired but whose measurements were made 20 days after clinical intervention. With DFA, we find on intact rats from the control group a crossover from non-stationary to stationary, long-range correlated fluctuations in arterial systolic blood pressure time series. This crossover indicates that baroreflex sets in for pressure control at a characteristic timescale. One day after surgery one finds that

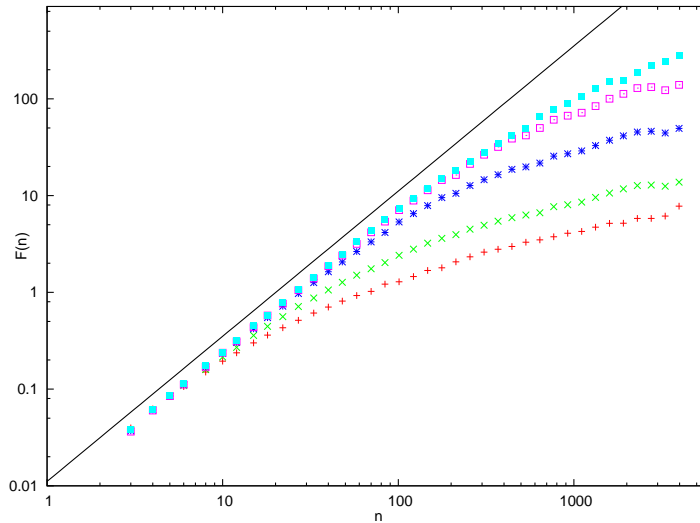


Figure 9. Detrended fluctuation analysis (DFA) of the artificial systolic blood pressure time series generated by the forced random walk model (equation 3). We plot 5 values of the sensitivity difference: $thr_s - thr_v = 3$ (red cross), $thr_s - thr_v = 5$ (green times), $thr_s - thr_v = 8$ (blue stars), $thr_s - thr_v = 11$ (pink empty squares) and $thr_s - thr_v = 15$ (cyan full squares). The sensitivity difference increase as the same the crossover scale. To guide the eye we show the curve with $\alpha = 1.5$ (black full line). A large threshold for the action of autonomous system forces also means that more information (afferent signals) needs to be integrated at NTS to respond to a change in blood pressure.

the feedback control, previously provided by baroreceptors, is impaired: no crossover is found, and pressure fluctuations are non-stationary. Nevertheless, after 20 days of surgical intervention we find evidence for physiological adaptation, and fluctuations scale in a fashion which is statistically similar to those from the time series of rats in the control group, only with the crossover from non-stationary to stationary fluctuations occurring at a larger timescale. We also design a model for baroreflex which has the same dynamical behavior of both normal and chronic SAD rats, qualitatively reproducing the crossover in the scaling of fluctuations. The main feature of the model is its self-inhibitory behavior, which illustrates the main principles underlying homeostatic control in living systems, and has been observed at very different organizational levels as an efficient mechanism for the maintenance of regularity in a fluctuating environment.

Acknowledgments

We thank A.Tavares Costa Jr. for a critical reading of the manuscript and an anonymous referee for suggestions significantly improving manuscript presentation. This work is partially supported by Brazilian Agencies CNPq, CAPES and FAPERJ.

References

- [1] F. Jacob and J. Monod. Genetic regulatory mechanisms in the synthesis of proteins. *J. Mol. Biol.*, 3:318–356, 1961.
- [2] M. A. Savageau. Comparison of classical and autogenous systems of regulation in inducible operons. *Nature*, 252:546–549, 1974.
- [3] A. Becskei and L. Serrano. Engineering stability in gene networks by autoregulation. *Nature*, 405:590–593, 2000.
- [4] J. Paulsson. Summing up the noise in gene networks. *Nature*, 427:415–418, 2004.
- [5] Y. Dublanche, K. Michalodimitrakis, Nico Kümmerer, Mathilde Foglierini, and Luis Serrano. Noise in transcription negative feedback loops: simulation and experimental analysis. *Mol. Syst. Biol.*, 2:41, 2006.
- [6] Hitomi Ogata, Kumpei Tokuyama, Shoichiro Nagasaka, Akihiko Ando, Ikuyo Kusaka, Naoko Sato, Akiko Goto, Shun Ishibashi, Ken Kiyono, Zbigniew R. Struzik, and Yoshiharu Yamamoto. Long-range negative correlation of glucose dynamics in humans and its breakdown in diabetes mellitus. *Am. J. Physiol. Regul. Integr. Comp. Physiol.*, 291(6):R1638–R1643, 2006.
- [7] Shunji Kishida, Koji Inoue, and Kunihiko Washio. Negative-feedback power stabilization in a mode-locked nd:yag laser. *Opt. Lett.*, 5:191–193, 1980.
- [8] Arthur C. Guyton and John E. Hall. *Textbook of Medical Physiology*. W.B. Saunders Company, 2000.
- [9] Adel K. Afifi and Ronald A. Bergman. *Functional Neuroanatomy, 2nd Edition (Lange Basic Science)*. McGraw-Hill Medical, 2005.
- [10] A. C. Guyton. Blood pressure control—special role of the kidneys and body fluids. *Science*, 252(5014):1813–1816, 1991.
- [11] L. B. Virginia and A. F. Sved. Pressure to change?: Re-evaluating the role of baroreceptors in the long-term control of arterial pressure. *Am. J. Physiol. Regul. Integr. Comp. Physiol.*, 288:R815–R818, 2005.
- [12] Gianfranco Parati, Giuseppe Mancia, Marco D. Rienzo, Paolo Castiglioni, Andrew J. Taylor, and Peter Studinger. Point:counterpoint: Cardiovascular variability is/is not an index of autonomic control of circulation. *J. Appl. Physiol.*, 101(2):676–682, 2006.
- [13] Thomas M. Coffman and Steven D. Crowley. Kidney in hypertension: Guyton redux. *Hypertension*, 51(4):811–816, 2008.
- [14] P. P. da S. Soares, A.C. Lucas da Nóbrega, M. R. Ushizima, and M. C. C. Irigoyen. Cholinergic stimulation with pyridostigmine increases heart rate variability and baroreflex sensitivity in rats. *Auton. Neurosci.*, 113(1):24–31, 2004.
- [15] S. Akselrod, D. Gordon, F. A. Ubel, D. C. Shannon, A. C. Barger, and R. J. Cohen. Power spectrum analysis of heart rate fluctuation: A quantitative probe of beat-to-beat cardiovascular control. *Science*, 213:220–222, 1981.
- [16] M. Pagani, F. Lombardi, S. Guzzetti, G. Sandrone, O. Rimoldi, and G. Malfatto. Power spectral density of heart rate variability as an index of sympatho-vagal interaction in normal and hypertensive subjects. *J. Hypertens.*, 2(S383-S385), 1984.
- [17] M. Pagani, V. Somers, R. Furlan, S. Dell’Orto, and G. Baselli. Changes in autonomic regulation induced by physical training in mild hypertension. *Hypertension*, 12:600–610, 1988.
- [18] W. Langewitz and H. Ruddle. Spectral analysis of heart rate variability under mental stress. *J. Hypertens. Suppl.*, 7(6):S32–33, 1989.
- [19] L. Bernardi, L. Ricordi, P. Lazzari, P. Solda, A. Calciati, and M. R. Ferrari. Impaired circadian modulation of sympathovagal activity in diabetes. a possible explanation for altered temporal onset of cardiovascular disease. *Circulation*, 86:1443–1452, 1992.
- [20] G. Mancia, G. Parati, P. Castiglioni, and M. di Rienzo. Effect of sinoaortic denervation on frequency-domain estimates of baroreflex sensitivity in conscious cats. *Am. J. Physiol. Heart. Circ. Physiol.*, 276:H1987–H1993, 1999.

- [21] C. K. Peng, J. Mietus, J. M. Hausdorff, S. Havlin, H. E. Stanley, and A. L. Goldberger. Long-range anticorrelations and non-gaussian behavior of the heartbeat. *Phys. Rev. Lett.*, 70(9):1343–1346, 1993.
- [22] A. Eke, P. Herman, L. Kocsis, and Kozak L. R. . Fractal characterization of complexity in temporal physiological signals. *Physiol. Meas.*, 23:R1–R38, 2002.
- [23] C. K. Peng, S. V. Buldyrev, S. Havlin, M. Simons, H. E. Stanley, and A. L. Goldberger. Mosaic organization of dna nucleotides. *Phys. Rev. E*, 49(2):1685–1689, 1994.
- [24] Z. Chen, P. Ch. Ivanov, Kun Hun, and H. E. Stanley. Effect of nonstationarities on detrended fluctuation analysis. *Phys. Rev. E*, 65(4):041107, 2002.
- [25] C. K. Peng, S. Havlin, H. E. Stanley, and A. L. Goldberger. Quantification of scaling exponents and crossover phenomena in nonstationary heartbeat time series. *Chaos*, 5(1):82–87, 1995.
- [26] J. C. Echeverría, B. R. Hayes-Gill, J. A. Crowe, M. S. Woolfson, and G. D. H. Croaker. Detrended fluctuation analysis: a suitable method for studying fetal heart rate variability? *Physiol. Meas.*, 25:763–774, 2004.
- [27] R. Karasik, N. Sapir, Y. Ashkenazy, P. C. Ivanov, I. Dvir, P. Lavie, and S. Havlin. Correlation differences in heartbeat fluctuations during rest and exercise. *Phys. Rev. E*, 66(6):062902, 2002.
- [28] A. Bunde, S. Havlin, J. W. Kantelhardt, T. Penzel, J.H. Peter, and K. Voigt. Correlated and uncorrelated regions in heart-rate fluctuations during sleep. *Phys. Rev. Lett.*, 85(17):3736–3739, 2000.
- [29] E. Rodriguez, J. C. Echeverria, and J. Alvarez-Ramirez. Detrended fluctuation analysis of heart intrabeat dynamics. *Physica A*, 384:429–438, 2007.
- [30] A. M. Schreihof and A. F. Sved. Use of sinoaortic denervation to study the role of baroreceptors in cardiovascular regulation. *Am. J. Physiol. Regul. Integr. Comp. Physiol.*, 266:R1705–R1710, 1994.
- [31] Thiago S. Moreira, Monica A. Sato, Ana C. Takakura, Jose V. Menani, and Eduardo Colombari. Role of pressor mechanisms from the nts and cvlm in control of arterial pressure. *Am. J. Physiol. Regul. Integr. Comp. Physiol.*, 289(5):R1416–R1425, 2005.
- [32] Ann C. Bonham, Chao-Yin Chen, Shin-Ichi Sekizawa, and Jesse P. Joad. Plasticity in the nucleus tractus solitarius and its influence on lung and airway reflexes. *J. Appl. Physiol.*, 101(1):322–327, 2006.
- [33] Chi-Sang Poon and Marina S. Siniaia. Plasticity of cardiorespiratory neural processing: classification and computational functions. *Respiration Physiology*, 122(2-3):83–109, 2000.
- [34] National Research Council. *Guide for the Care and Use of Laboratory Animals*. National Academy Press, Washington D.C., 1996.
- [35] E. M. Krieger. Neurogenic hypertension in the rat. *Circ. Res.*, 15:511–521, 1964.
- [36] P. P. da S. Soares, C. S. Port, F. M. F. Abdalla, R. N. De La Fuente, E. D. Moreira, E. M. Krieger, and M. C. Irigoyen. Effects of rat sinoaortic denervation on the vagal responsiveness and expression of muscarinic acetylcholine receptors. *J. Cardiovasc. Pharmacol.*, 47(3):331–336, March 2006.
- [37] S. Havlin, L. A. Amaral, Y. Ashkenazy, A. L. Goldberger, P. Ch. Ivanov, C. K. Peng, and H. E. Stanley. Application of statistical physics to heartbeat diagnosis. *Physica A*, 274:99–110, 1999.
- [38] D. T. Schmitt and P. C. Ivanov. Fractal scale-invariant and nonlinear properties of cardiac dynamics remain stable with advanced age: A new mechanistic picture of cardiac control in healthy elderly. *Am. J. Physiol. Regul. Integr. Comp. Physiol.*, 293:R1923–R1937, 2007.
- [39] A. Bashan, R. Bartsch, J. W. Kantelhardt, and S. Havlin. Comparison of detrending methods for fluctuation analysis. *Physica A*, 387(21):5080–5090, 2008.
- [40] Kun Hu, Plamen Ch. Ivanov, Zhi Chen, Pedro Carpena, and H. Eugene Stanley. Effect of trends on detrended fluctuation analysis. *Phys. Rev. E*, 64(1):011114, 2001.
- [41] J. W. Kantelhardt, E. Koscielny-Bunde, H. H. A. R. S. Havlin, and A. Bunde. Detecting long-range correlations with detrended fluctuation analysis. *Physica A*, 295:441–454, 2001.
- [42] M. Latka, M. Glaubic-Latka, D. Latka, and B.J. West. Fractal rigidity in migraine. *Chaos*,

- Solitons & Fractals*, 20(1):165–170, 2004.
- [43] William Press, Saul Teukolsky, William Vetterling, and Brian Flannery. *Numerical Recipes in C*. Cambridge University Press, Cambridge, UK, 2nd edition, 1992.
 - [44] Atsunori Kamiya, Toru Kawada, Kenta Yamamoto, Daisaku Michikami, Hideto Ariumi, Kazunori Uemura, Can Zheng, Syuji Shimizu, Takeshi Aiba, Tadayoshi Miyamoto, Masaru Sugimachi, and Kenji Sunagawa. Resetting of the arterial baroreflex increases orthostatic sympathetic activation and prevents postural hypotension in rabbits. *The Journal of Physiology*, 566(1):237–246, July 2005.
 - [45] Smyth H.S., Sleight P., and Pickering G.W. Reflex regulation of arterial pressure during sleep in man. a quantitative method of assessing baroreflex sensitivity. *Circ. Res.*, 24:109–121, 1969.
 - [46] R. Carretta, M. Bardelli, G. Bulli, B. Fabris, F. Fischetti, F. Vran, P. Rizzini, V. D’Onofrio, F. Bamfi, and L. Campanacci. An ultrasonographic method to measure the sensitivity of the baroreflex in clinical practice: application to pharmacological studies. *J Hypertens Suppl*, 9:S33–36, Dec 1991.
 - [47] Maria Teresa La Rovere, Gian Domenico Pinna, and Grzegorz Raczak. Baroreflex sensitivity: Measurement and clinical implications. *Ann. Noninvasive Electrocardiol.*, 13(2):191–207, 2008.
 - [48] L. M. McDowall and R. A. Dampney. Calculation of threshold and saturation points of sigmoidal baroreflex function curves. *Am. J. Physiol. Heart. Circ. Physiol.*, 291(4):H2003–H2007, 2006.
 - [49] Zbigniew R. Struzik, Junichiro Hayano, Seiichiro Sakata, Shin Kwak, and Yoshiharu Yamamoto. 1/f scaling in heart rate requires antagonistic autonomic control. *Phys. Rev. E*, 70(5):050901, 2004.
 - [50] C. E. C Galhardo, T. J. P. Penna, M. A. de Menezes, and P.P. Soares. unpublished.